Engineering Structures 168 (2018) 399–404

Contents lists available at ScienceDirect

Engineering Structures

journal homepage: www.elsevier.com/locate/engstruct

Optimal seismic retrofitted RC column distribution for an existing school building

Hyunsu Seo[a], Jinsup Kim[b], Minho Kwon[b,*]

[a] Dept. of Civil Engineering, University of Texas at Arlington, Arlington, TX 76019, USA
[b] Dept. of Civil Engineering, ERI, Gyeongsang National University, Jinju 52828, South Korea

ARTICLE INFO

Keywords:
Optimization
RC column seismic retrofitting
Time-history dynamic analysis
School building
Location of seismic retrofitting

ABSTRACT

Seismic retrofit technology has been significantly developed to reduce building damage during earthquakes. However, earthquakes are unpredictable natural disasters that should be dealt with flexibly. Hence, the seismic retrofitting method should be independently studied. In this study, the minimum number and the location of seismic retrofitted reinforced concrete columns required for school buildings in service are derived through an optimization technique. A time-history dynamic analysis of the frame structure comprising columns and beams is conducted using a three-dimensional finite element model to obtain empirical results. The study subject is a school building, which is a three-story RC structure with non-seismic details consisting of 62 RC columns on each floor (i.e., a total of 186 columns). The optimization analysis showed that retrofitting only 60.2% of the columns could withstand a peak ground acceleration of 0.2 g applied at the shear critical regions at both column ends.

1. Introduction

Many engineers established seismic design criteria for structures to reduce the damage caused by seismic activities. Considering worldwide population densities and social infrastructure systems, the most damaging earthquakes have frequently occurred in California in the western United States. Following the severe destruction or collapse of several hospital buildings during the San Fernando earthquake in 1971, California passed a bill [1] specifying that hospital buildings must remain functional after earthquakes. The follow-up bill in 1994, which was called “SB 1953” [2], stated that all key facilities of the society, including hospitals at the secondary healthcare facility level or higher and school buildings, must be evaluated for seismic performance and retrofitted accordingly. The seismic retrofitting of general buildings has been significantly improved. Starting from FEMA 273 [3], the Vision 2000 seismic retrofitting standard (SEAOC 1995, [4]) established guidelines for the seismic retrofitting of existing buildings and the performance-based design concept. ASCE41-06 [5] is being widely used today based on this and through FEMA 356 [6]. Buildings in the United States have been retrofitted according to the current seismic design and retrofitting criteria although technological evolution may require additional standards.

While design techniques for seismic retrofitting have been improved, the actual construction site performance significantly varies depending on proficiency. Seismic performance may also differ. Therefore, overcoming these shortcomings is necessary to develop retrofitting techniques that would lead to increased work efficiency and produce standardized retrofitting materials to enable unskilled workers to perform fast and effective work. During an earthquake, the RC columns of a structure are generally subjected to lateral loads (shear loads) together with axial loads. Column failures may be caused by the lack of shear strength, bending strength, or ductility [7]. Studies on seismic retrofitting materials currently focus on these factors. The RC column seismic retrofitting material developed by Seo, Kim, and Kwon [8] is particularly considered excellent in terms of shear strength, ductility, and work efficiency.

Therefore, the present study uses an optimization process to identify the most efficient locations to apply seismic retrofitting to RC columns in school buildings using the RC column seismic retrofitting material developed by Seo et al. [8].

2. Optimization method

This study employed the ant colony optimization method, which has been attempted for utilization in optimization studies. This study used this optimization method to present an algorithm that could derive optimal results through a dynamic time-history analysis.

Abbreviations: ACO, ant colony optimization; GFRP, glass fiber-reinforced polymer

* Corresponding author.
E-mail addresses: jinsup.kim@gnu.ac.kr (J. Kim), kwonm@gnu.ac.kr (M. Kwon).

https://doi.org/10.1016/j.engstruct.2018.04.098
Received 8 September 2017; Received in revised form 15 February 2018; Accepted 30 April 2018

2.1. Ant colony optimization

Various optimization techniques have been developed over the last several decades as a result of many studies on the optimization of discrete structures using improved computer technology. In the 1990s, Rajeev and Krishnamoorthy [9] proposed a discrete structure optimization method using genetic algorithms. Shih [10] improved and applied fuzzy theory. Park et al. [11] applied a discrete optimization technique to the optimal design of steel frame structures. Meanwhile, Lee et al. [12] attempted to optimize discrete structures using the harmony search method.

While these studies were conducted, Dorigo and Caro [13] developed a new algorithm, called ant colony optimization (ACO). ACO is based on random combinations obtained by observing ant behavior and is a meta-heuristic technique that imitates a natural phenomenon. The other existing meta-heuristic techniques, including genetic algorithms, have difficulty in selecting parameters and require considerable effort to find the optimal solution because selecting the wrong parameters may lead to failure in finding a solution. However, the ant algorithm significantly reduces the time and effort required to select parameters because it is relatively less sensitive to parameter selection compared to other meta-heuristic techniques.

Lee and Han [14] showed that the optimal design performed by the ant algorithm is superior to other optimization techniques. They applied 41 types of cross-sections to a plane truss structure with 10 members. They also applied structure weight to optimal design problems. Compared with the results of the genetic algorithm and CONMIN optimization software, which are representative meta-heuristic optimization techniques, the optimal design weight using the ant algorithm is the smallest (Table 1), indicating its excellent performance.

For a problem with numerous system search paths, a system user without sufficient knowledge of the ant algorithm can still easily use it because modifying subsequent parameters becomes unnecessary once the initial parameters are set [19]. The optimization problems herein are solved using the ant algorithm because of the system advantages.

2.2. ACO optimal algorithm with non-linear time-history analysis

Efficient and systematic procedures are required for the optimization process of selecting the optimal number and the location of the developed seismic retrofitting material to be applied to non-seismic school buildings in service to achieve the objective of the given optimal solution. The discrete optimization for the structure and linking it to the structure analysis software particularly required a more careful attention. The first step in this process was to determine the overall optimization analysis algorithm for efficient computation. The non-linear time-history analysis used the FE analysis commercial software and, hence, was linked to the ACO software. An algorithm was also designed for the two software programs to interact with each other (see Supplementary Fig. 1).

3. Numerical modeling

3.1. Verification of the FEM analysis model by the test of Seo et al. [8]

This study used glass fiber-reinforced polymer (GFRP) for the RC column seismic retrofitting developed by Seo, Kim, and Kwon [8]. Therefore, the finite element model of the retrofitted RC column used in this study was verified through a comparison with the experimental results of the performance evaluation.

Table 1
Optimum values of different methods [14].

Benchmarking data	Weight (kN)
Genetic algorithm [15]	24.78148
CONMIN [16]	24.80846
Genetic algorithm [17]	24.43074
ACO [18] (Camp, 2004)	24.34797

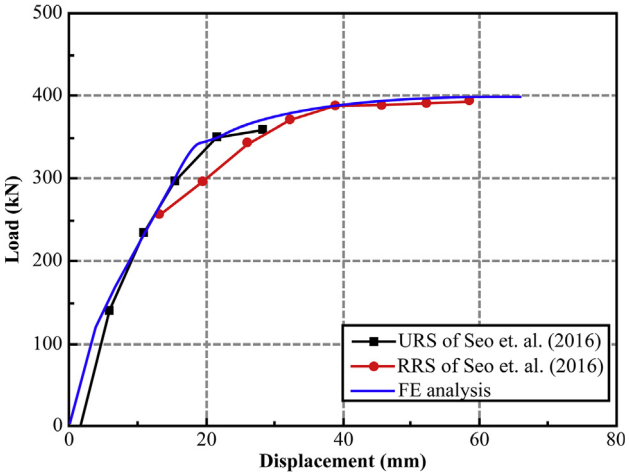

Fig. 1. Comparison with tests (Seo et al. [8]) and FE analysis for the load–displacement curves.

The same RC frame structure as the specimen was modeled using the beam element. The commercial software LS-DYNA was used for the structure analysis. Meanwhile, Hughes–Liu was used as the beam element, and CONCRETE_EC2 was utilized as the material model. The same material properties as those used in the experiment were provided [16]. Fig. 1 shows the analysis results (load–displacement curves). The envelope curve of the non-retrofitted URS specimen and that of the retrofitted RRS specimen were compared. The FE analysis showed that the initial stiffness agreed with the experimental results, and the behavior was almost similar to that of the RRS specimen even after yielding. The yield point almost agreed with that of the URS specimen, but was somewhat different from that of the RRS specimen. The experiment was conducted with an already damaged specimen; hence, the yield point was different from that in the case of the URS. The finite element model used herein showed the same results with the URS specimen from the early behavior to the yield point. The ductile behavior was similar to that of the RRS specimen. Therefore, the validity of the proposed method is thought to be verified because it reached the performance level of both specimens.

The strain at the time of collapse was derived from the verified numerical analysis. The displacements of the URS and RRS specimens at the time of collapse were 28.6 mm and 65.2 mm, respectively. The strains at the time of collapse were 0.00365 and 0.00573 in the numerical analysis. Therefore, the limit strain of the RC column was determined as 0.00365 for non-retrofitting and 0.00573 for retrofitting, which were set as the allowable strains of the RC column.

3.2. Geometry and load of school building

The target school building was a three-story elementary school with a floor height of 3.5 m and a long-side length of 90 m with 20 same spans 4.5 m in length. Its short-side direction was asymmetrical with one side having a 2.4 m span and two 3.6 m spans and the other side having four 2.4 m spans. Fig. 2 shows the floor plan. The school building had columns with five different types of cross-sections. Table 2 presents each cross-section. The applied load was in accordance with the design document of the school building. Both the dead and live loads were assumed as the working load as the structure in service was being evaluated. Table 3 presents the loads applied to each girder and beam.

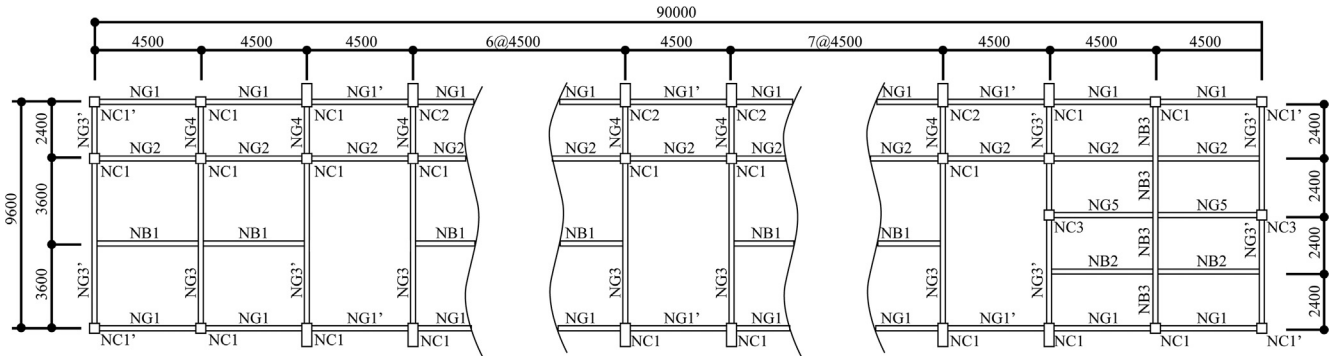

Fig. 2. Floor plan of the school building (unit: mm).

3.3. Three-dimensional (3D) numerical modeling for non-linear time-history dynamic analysis

The RC frame structure was modeled using Hughes–Liu beam elements to analyze the school building using the LS-DYNA structure analysis software [20]. A total of 3249 nodes and 3540 elements were used. Placing retrofitting materials in the shear critical regions was the most efficient. Hence, the retrofitting material used in this frame structure modeling was also placed in the shear critical regions. The length corresponding to the shear critical regions of each member was set as the minimum length of the beam element used. The retrofitting material in the modeling was placed on both ends of a column. Fig. 3 shows the 3D modeling view using the LS-DYNA software. The black elements in the figure were the targets of the seismic retrofitting.

3.4. Selection of the input earthquake motion for the dynamic analysis

The seismic waves directly or simply amplified from the observed seismic waves can be used for the seismic analysis and design. However, the artificial earthquake time history generated in accordance with the design spectrum was generally used because the design earthquake given as the response spectrum was difficult to cover in all frequency domains [21]. The stochastic method is a universal method for generating the artificial earthquake time history. This method equally generates white noise with all frequency components and adjusts the amplitude of each frequency component to generate a target spectrum. This method uses the phase angles extracted from the measured seismic waves and, sometimes, uses only the amplitude adjustment method to reflect the actual seismic characteristics [22]. This stochastic method can converge to the target spectrum through several iterations and freely adjust the seismic wave duration. In addition, the method can generate various seismic waves without cross-correlations by randomly

Table 3
Load on structure (unit: N/mm).

Member	G1Y3	G1Y1	G2	G3	NC4	B1
Dead load	4.75	6.71	11.47	7.91	4.89	3.88
Live load	3.42	4.82	8.24	5.67	3.51	2.24

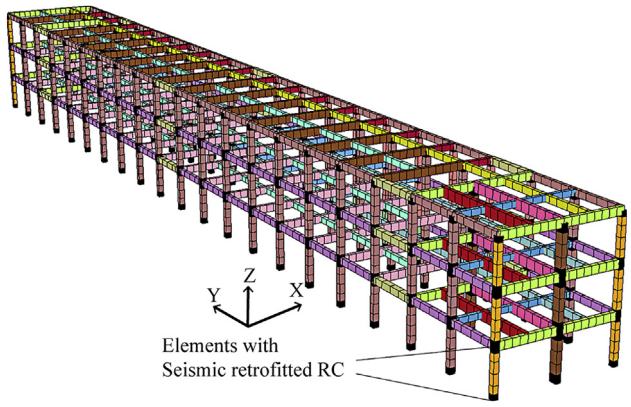

Fig. 3. 3D modeling view of the RC frame for the school structure.

Table 2
Section properties of members (unit: mm).

Member		NC1	NC1′	1C2	2&3C2	NC3
Dimension		400 × 450	400 × 400	400 × 400	400 × 400	600 × 400
Main bar		6-D19	6-D19	6-D19	4-D19	10-D19
		2-D16	2-D16			
Hoop		D10@300	D10@300	D10@300	D10@300	D10@300
Member		1&2G1	3G1	NG1′	1&2G2	1&2G3
		3G2				
Dimension		300 × 500	300 × 500	450 × 500	300 × 500	300 × 600
Main Bar	Top	2-D16	2-D16	2-D19	2-D16	2-D22
	Bottom	3-D16	2-D16	3-D19	4-D16	6-D22
Stirrup		D10@300	D10@300	D10@300	D10@300	D10@300
Member		3G3	NG3′	1 & 2G4	3G4	NG5
Dimension		300 × 600	300 × 600	300 × 450	400 × 450	330 × 700
Main Bar	Top	2-D19	2-D19	2-D22	2-D19	2-D22
	Bottom	6-D19	2-D19	4-D22	4-D19	6-D22
Stirrup		D10@300	D10@300	D10@300	D10@300	D10@300
Member		NB1	NB2	NB3	–	–
Dimension		300 × 450	330 × 700	300 × 450		
Main Bar	Top	2-D22	2-D22	2-D19		
	Bottom	6-D22	6-D22	2-D19		
Stirrup		D10@300	D10@300	D10@300		

determining the phase angles of each frequency.

This method was performed in the frequency domain. Hence, the frequency characteristics of the seismic waves were those of the stationary waves that did not change over time. However, the time history of the observed seismic waves had non-stationary characteristics, in which the frequency characteristics changed over time. Moreover, implementing this time history using the method of generating seismic waves in the frequency domain was difficult. Therefore, a method of directly modifying the measured time history in the time domain was recently developed to directly reflect not only the non-stationary wave characteristics, but also the various characteristics of actual earthquakes [23].

ASCE 43-05 [24] recommends using the artificial time history stochastically generated by adjusting the amplitude of the frequency components in the analysis of the linear seismic responses. Meanwhile, the recorded seismic waves were used in the analysis of the non-linear seismic responses. Although 30 input seismic waves must be used to obtain the response distribution with statistical significance, ASCE 4-98 [25] recommends using three or more seismic waves. Therefore, this study analyzed the actual seismic waves and applied appropriate earthquakes.

The analysis of the natural seismic waves based on the frequency band using the Fourier spectrum showed that the Kobe, San Fernando, and Imperial Valley earthquakes were suitable for deriving the optimal retrofitting material for the school building. However, the Imperial Valley earthquake was not significantly influential when applied to the school building because it was dominated by high frequencies (9 Hz). Therefore, only the Kobe and San Fernando earthquakes were considered.

The Kobe earthquake was predominant at a frequency of approximately 1 Hz, whereas the San Fernando earthquake was predominant at approximately 4 Hz. The most significant characteristic from their acceleration–time histories was their different durations. The Kobe earthquake had a longer duration than the San Fernando earthquake. The diversity of the seismic waves applied to the non-linear dynamic analysis (time-history analysis) can be judged as secured. Fig. 4 shows the final selected acceleration–time history curve. The peak ground acceleration (PGA) of each natural seismic wave was 0.6114 and 0.0321 for the Kobe and San Fernando earthquakes, respectively.

4. Optimization result

The optimal number and the location of the retrofitting materials required for the school building columns in South Korea were derived through an optimization technique using the GFRP seismic retrofitting material employed in this study. The number of the retrofitting material represented the number of retrofitted columns. The retrofitting material was installed at both ends of a column.

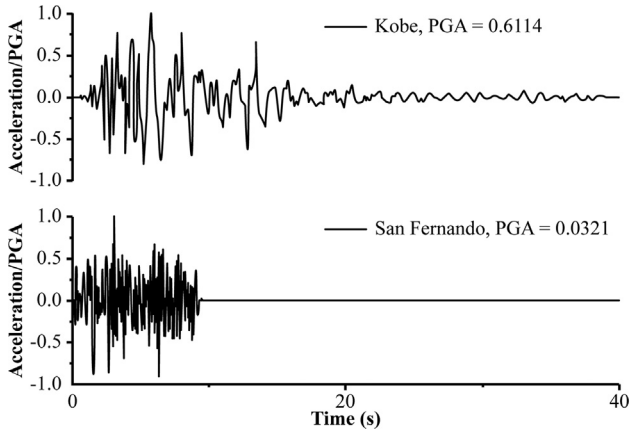

Fig. 4. Acceleration–time histories selected for the dynamic analysis.

The building has an asymmetric structure, and an actual earthquake can occur in various directions rather than only in one direction. Therefore, the optimization problem with different forcing directions was planned to derive the optimal location of the retrofitting material according to the directions of the time-history forcing. Moreover, although the building structure had non-seismic details, it could bear an increase of up to 0.12 g of PGA in the Kobe earthquake even without an additional retrofitting material, which was why it was applied from 0.13 g PGA.

4.1. Optimality criteria of the optimization problem

The objective function in this study comprised the number of columns to be retrofitted in the RC structure and their locations. The seismic design criteria and the limit condition of the column members derived from the experiment were set as the constraint conditions.

The first objective function was set as the number of columns to be retrofitted. Its constraint condition is shown in Eq. (1).

$$\begin{aligned} &\text{Minimize:} \quad \Psi(R_e) = \sum_{e=1}^{ncel} R_e \\ &\text{subject to:} \quad |\varepsilon_{CRallow}/\varepsilon_{Ce}| \geqslant 1, \quad |\varepsilon_{CUallow}/\varepsilon_{Ce}| \geqslant 1, \quad |\delta_{allow}/\delta_{Ce}| \geqslant 1 \end{aligned} \tag{1}$$

where Ψ is the objective function of the optimization problem; R_e is the column to be retrofitted; $R_e = 0$ is a non-retrofitted column; $R_e = 1$ is a retrofitted column making the objective function minimum; *ncel* is the total number of column members; $\varepsilon_{CRallow}$ and $\varepsilon_{CUallow}$ are the allowable strains of the retrofitted and non-retrofitted column members, respectively; ε_{Ce} is the strain of each column member; δ_{allow} is the allowed inter-story displacement; and δ_{Ce} is the inter-story displacement generated from each column member.

The second objective function was set as the inter-story displacement of the column. Its constraint condition is shown in Eq. (2). The number of retrofitted columns was set as a constraint condition, such that the number of the retrofitted columns derived above could remain constant.

$$\begin{aligned} &\textit{Minimize:} \quad \Psi(\delta_{Ce}) = \max(|\delta_{Ce}|) \\ &\textit{subjectto:} \quad R_{CUe} = 0, |\varepsilon_{CRallow}/\varepsilon_{Ce}| \geqslant 1, |\varepsilon_{CUallow}/\varepsilon_{Ce}| \geqslant 1 \end{aligned} \tag{2}$$

where δ_{Ce} is the inter-story displacement generated from each column member, and the objective function Ψ is the maximum inter-story displacement of the inter-story displacements of each column. R_{CUe} is the non-retrofitted column derived from the process of minimizing the number of retrofitting materials and set as a constraint condition, such that the total number of retrofitted columns could remain constant.

4.2. Performance of the optimization and optimal number of retrofitted RC columns

The optimization histories shown in Fig. 5 illustrated that convergence was generally reached through more than 200 iterations, and this pattern appeared in all optimization problems in the same manner. Therefore, in conclusion, the technique combining the optimization technique and the time-history analysis resulted in a reliable performance.

While the final number of iterations in the optimization process was approximately 600, the number of iterations increased with the PGA, thereby showing a maximum difference of 100 iterations. This result was obtained because the number of cases that must be searched also increased in the optimization process for determining the placement of the retrofitted columns if the number of retrofitted columns increased. However, no significant difference was found in the number of iterations, and the patterns remained constant. Hence, the optimization performance was satisfactory.

The number of retrofitted columns derived by the optimization

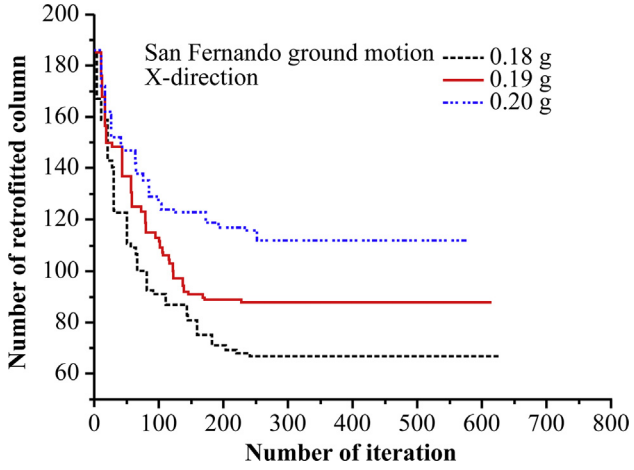

Fig. 5. Optimization histories.

analysis increased with the PGA. The same tendency occurred when forcing was applied in different directions. The number of retrofitted columns varied from 60 to 100 according to the PGA and increased by 20 for every 0.1 increase in the PGA. The fact that the same tendency occurred while a different PGA was applied according to the forcing directions indicated that the strength of the structure varied according to the forcing directions. However, its increasing or decreasing pattern remained constant, thereby indicating the necessity to consider the forcing direction in addition to the seismic characteristics considered in the general seismic design.

Supplementary Table 1 shows the number of retrofitted columns and the number of iterations derived by the optimization analysis.

4.3. Distribution of the optimal seismic retrofitted RC columns

The first floor required the highest number of retrofitted columns, and the number decreased as the floor level increased. The number of retrofitted columns on the third floor was significantly different from those on the first and second floors. The seismic load was mostly absorbed by the first and second floors. Hence, a higher number of retrofitted columns were required on those floors. The seismic load was focused on the first floor and not effectively distributed.

The placement of the retrofitted columns was slightly different according to the forcing directions. The outer and center columns in the X-direction forcing required considerable retrofitting. Meanwhile, the outer columns in the 45° direction and Y-direction forcing required more retrofitting, while the center columns required less. Retrofitting was not performed well in adjacent columns. The first and second floors for the outer column retrofitting showed similar location patterns. Meanwhile, those for the center column retrofitting showed different location patterns. The load distribution seemed enhanced by these location patterns.

The retrofitted column placement in the X-direction showed that the inner columns also required retrofitting. In general design, the cross-section detail for the inner columns is designed to be large because of the burden of the live load and the position of these columns. The burden of the live load is significant during an earthquake. Therefore, appropriate seismic retrofitting is also required for the inner columns. Supplementary Fig. 2 shows the placement of the retrofitted columns on each floor.

5. Conclusions

This study derived the optimal number and the location of retrofitted RC columns by linking the optimization technique with a 3D non-linear time-history analysis. Various results were obtained by performing the 3D non-linear dynamic analysis. Moreover, reliable optimization results were acquired using the ACO optimization technique. The main contributions of the study are as follows:

(1) An algorithm that combines the ACO technique and the 3D non-linear time-history analysis is proposed.
(2) The optimization using the ACO technique shows that reliable results could be derived.
(3) The structure strength varies according to the forcing direction of the earthquake. Its deviation is also large. The strength along the strong axis (Y-axis) is high because of the large number of spans. The strength significantly varies according to the forcing direction in school buildings with asymmetric loads and structures. Hence, the forcing direction must be closely examined, and the risk for the weak axis (X-axis) with fewer spans must be recognized.
(4) The seismic material proposed in this study must be installed in over 50% of the total columns for non-seismic school buildings to meet the current seismic design criteria.
(5) Further retrofitting is required for a higher PGA, which determines the strength of the seismic waves, for the weak axis (X-axis) with fewer spans and for lower floor levels. Retrofitting the outer columns is more effective than retrofitting the inner columns.
(6) A staggered positioning of the retrofitted columns over a wide area is more effective than continuous positioning. Applying different retrofitting locations to each floor contributes to economic benefits.

Acknowledgements

This research was supported by a grant (2017-MOIS31-002) from the Fundamental Technology Development Program for Extreme Disaster Response funded by the Korean Ministry of Interior and Safety (MOIS).

Conflict of interest

none

Appendix A. Supplementary material

Supplementary data associated with this article can be found, in the online version, at http://dx.doi.org/10.1016/j.engstruct.2018.04.098.

References

[1] Mualchin L. History of modern earthquake hazard mapping and assessment in California using a deterministic or scenario approach. Pure Appl Geophys 2011;168(3–4):383–407.
[2] Alesch DJ, Petak WJ. Seismic retrofit of California hospitals: implementing regulatory policy in a complex and dynamic context. Nat Hazards Rev 2004;5(2):89–96.
[3] FEMA. NEHRP guidelines for the seismic rehabilitation of buildings (FEMA 273). Washington, D.C.: Building Seismic Safety Council; 1997.
[4] Structural Engineers Association of California (SEAOC). Vision 2000: performance based seismic engineering of buildings. Sacramento, CA: SEAOC; April 1995.
[5] ASCE. Seismic rehabilitation of existing buildings (ASCE/SEI 41–06). Reston, Virginia: ASCE; 2007.
[6] FEMA. Prestandard and commentary for the seismic rehabilitation of buildings (FEMA 356). Reston, Virginia: ASCE; 2000.
[7] Priestley MJN, Seible F. Design of seismic retrofit measures for concrete and masonry structures. Constr Build Mater 1995;9(6):365–77.
[8] Seo H, Kim J, Kwon M. Evaluation of damaged RC columns with GFRP-strip device. J Compos Constr 2016;20(4):04015089.
[9] Rajeev S, Krishnamoorthy CS. Discrete optimization of structures using genetic algorithms. J Struct Eng 1992;118(5):1233–50.
[10] Shih CJ. Fuzzy and improved penalty approaches for multiobjective penalty approaches for multiobjective mixed-discrete optimization in structural systems. Comput Struct 1997;63(3):559–65.
[11] Park SE, Park MH, Kwon MH, Chang CH. Discrete optimum design of steel framed structures subjected to deformed panel zone. J Comput Struct Eng Inst Korea 2002 15(2):315–27.
[12] Lee KS, Geen ZW, Lee SH, Bae KW. The harmony search heuristic algorithm for discrete structural optimization. Eng Optim 2005;37(7):663–84.

[13] Dorigo M, Di Caro G. The ant colony optimization meta-heuristic. New ideas in optimization. London: McGraw Hill; 1999, p. 12–32.
[14] Lee SJ, Han WD. Truss size optimization using ant colony optimization algorithm. J Archit Inst Korea: Struct Constr 2011;27(8):21–8.
[15] Camp C, Shahram P, Guozhong C. Optimized design of two-dimensional structures using a genetic algorithm. J Struct Eng 1998;124(5):551–9.
[16] Belegundu AD. A Study of mathematical programming methods for structural optimization. Doctoral dissertation, University of lowa, lowa City, IA.
[17] Ghasemi MR, Hinton E, Wood RD. Optimization of trusses using genetic algorithms for discrete and continuous variables. Eng Comput 1999;16(3):272–303.
[18] Camp CV, Bichon BJ. Design of space trusses using ant colony optimization. J Struct Eng 2004;130(5):741–51.
[19] Lee SY, Park YH, Lee JH. The development of a shortest route search demonstration system for the home delivery using ant algorithm: limiting to Yangyang Province. J Korea Ind Inf Syst Res 2007;12(4):89–96.
[20] Sedek F, Main JA, Lew HS, Bao Y. Testing and analysis of steel and concrete beam–column assemblies under a column removal scenario. J Struct Eng 2011;137(9):881–92.
[21] Hancock J, Watson-Lamprey J, Abrahamson NA, Bommer JJ, Markatis A, McCoy E, et al. An improved method of matching response spectra of recorded earthquake ground motion using wavelets. J Earthq Eng 2006;10(1):67–89.
[22] Mukherjee S, Gupta VK. Wavelet-based generation of spectrum-compatible time-histories. Soil Dyn Earthq Eng 2002;22(9):799–804.
[23] Giaralisa A, Spanos PD. Wavelet-based response spectrum compatible synthesis of accelerograms — Eurocode application (EC8). Soil Dyn Earthq Eng 2009;29(1):219–35.
[24] ASCE. Seismic design criteria for structures, systems, and components in nuclear facilities (ASCE 43–05). Reston, Virginia: ASCE; 2005.
[25] ASCE. Seismic analysis of safety-related nuclear structures and commentary (ASCE 4–98). Reston, Virginia: ASCE; 2000.